

UNCLASSIFIED

Defense Technical Information Center  
Compilation Part Notice

ADP015027

TITLE: Instabilities in Inductive Discharges with Electronegative Gases

DISTRIBUTION: Approved for public release, distribution unlimited

This paper is part of the following report:

TITLE: International Conference on Phenomena in Ionized Gases [26th]  
Held in Greifswald, Germany on 15-20 July 2003. Proceedings, Volume 4

To order the complete compilation report, use: ADA421147

The component part is provided here to allow users access to individually authored sections of proceedings, annals, symposia, etc. However, the component should be considered within the context of the overall compilation report and not as a stand-alone technical report.

The following component part numbers comprise the compilation report:

ADP014936 thru ADP015049

UNCLASSIFIED

# Instabilities in inductive discharges with electronegative gases

P. Chabert, H. Abada, and J.-P. Booth  
LPTP, Ecole Polytechnique, 91128 Palaiseau cedex, France

A.J. Lichtenberg, M.A. Lieberman, A. M. Marakhtanov  
Department of EECS, UC Berkeley, Berkeley CA, USA

*Relaxation oscillations in charged particle densities are seen in low-pressure electronegative inductive discharges, in the neighborhood of the transition between lower power capacitive operation and higher power inductive operation. The region of oscillatory behavior in both pressure and power increases as the plasma becomes more electronegative. Charged particle and free radical dynamics were investigated experimentally. A global model was developed which allowed to determine the parameters governing the transition to instability.*

## 1. Introduction

Instabilities in electronegative discharges have been studied in high-pressure dc glows [1-3], in rf capacitive discharges [4] and recently in low-pressure inductive discharges [5,6]. An inductive discharge can exist in two modes: the capacitive (E) mode, for low power, and the inductive (H) mode, for high power. As the power is increased, transitions from capacitive to inductive modes (E-H transitions) are observed [7,8]. When operating with electropositive gases the transition occurs at a given power, and the discharge is always stable. In contrast, when operating with electronegative gases, the transition is usually unstable, and a wide range of powers exist where the discharge oscillates between E and H modes [5,6,9]. The relaxation oscillations in this E-H transition cause charged particle density, electron temperature and plasma potential modulations. The free radical concentration may also oscillate if the frequency is low, as observed by laser induced fluorescence in a  $\text{CF}_4$  inductive discharge.

## 2. Experiments in $\text{CF}_4$ and $\text{SF}_6$

We have studied two different systems. The first device, located in Berkeley (USA), is a planar TCP, 30 cm in diameter and 19 cm long, working with  $\text{Ar}/\text{SF}_6$  gas mixtures. The coil is powered by 13.56 MHz rf power supply through a match box. The second device, located in the Ecole Polytechnique (France), is also a TCP (same diameter but 6 cm long) working with  $\text{CF}_4$  gas. In both systems, oscillations are seen in charged particle density, electron temperature and plasma potential using probes and OES measurements. When increasing power, we see a low power transition to enter the unstable region, and then an upper transition to a stable inductive mode as seen in figure 1. The instability windows get smaller as the argon partial pressure increases. It is also important to mention that a change in the matching network settings usually leads to a change in the frequency.

The frequency of the oscillations lies between 5 and 100 kHz for  $\text{SF}_6$ , and are about 30 times smaller for  $\text{CF}_4$  (see figure 2). This is predicted by theory and is mainly due to the fact that the attachment coefficient in  $\text{CF}_4$  is a

lot smaller than in  $\text{SF}_6$ , although there are some second order effects.

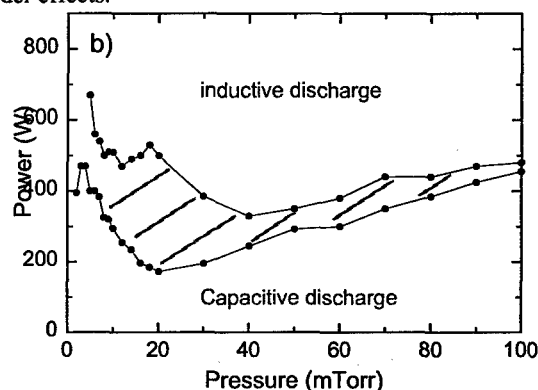


Figure 1: Instability window in (1:1)  $\text{Ar}/\text{SF}_6$  mixture.

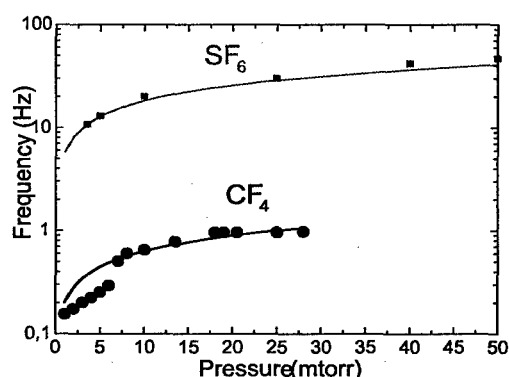


Figure 2: Instability frequencies versus pressure.

Results presented figure 3 for  $\text{Ar}/\text{SF}_6$  show that the electron and ion dynamics are different. This was not studied in  $\text{CF}_4$  since probe measurements are difficult in polymerizing chemistries. The electron density typically changes by a factor of 25, with fast rise and decay times. Over the same time, the ion densities only change by a factor of five and exhibit slower rise and decay times. Positive and negative ion densities decay at the same rate, which suggests that the ion losses are mainly due to mutual recombination.

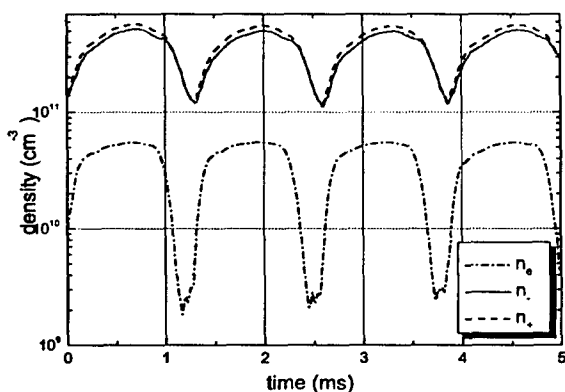


Figure 3: Densities vs time in (1:1)Ar/SF<sub>6</sub> mixture.

The free radical dynamics were investigated using space and time-resolved laser-induced fluorescence. The CF and CF<sub>2</sub> radical densities are strongly modulated during low-frequency instabilities, i.e. at low pressure. Several mechanisms were examined both from experimental and model results. Chemical reactions (either in the gas phase or at the wall) seem to be mainly responsible for the radical density fluctuations. Gas heating effects, observed previously in the inductive mode, probably make some contribution to the radical dynamics, but do not explain the major part of the observed time variations.

### 3. Theory

A global model has been developed to describe the instability [6,9]. This model is based on three differential equations: the particle and energy balance equations.

$$\begin{aligned} \frac{dn_e}{dt} &= n_e n_g K_{iz} + n_- n_g^* K_{det} - n_e n_g K_{att} - \Gamma_e \frac{A}{V} \\ \frac{dn_-}{dt} &= n_e n_g K_{att} - n_- n_g^* K_{det} - n_- n_+ K_{rec} - \Gamma_- \frac{A}{V} \\ \frac{d}{dt} \left( \frac{3}{2} n_e T_e \right) &= P_{abs} - P_{loss} \end{aligned}$$

These equations can be integrated considering quasi-neutrality in the plasma volume and at the walls to produce the dynamical behavior. However, to better understand the physics, one can look at equilibrium curves, i.e. setting  $dn_e/dt = 0$ ,  $dn_-/dt = 0$ ,  $dT_e/dt = 0$ , and examine the stability in the  $n_-(n_e)$  phase plane. In figure 4d the phase space representation of  $dn_e/dt = 0$  (dashed line) is shown in the  $n_-$  vs  $n_e$  plane. "Below" the dashed line,  $dn_e/dt$  is positive. We also plot (dot-dashed line) the equation for  $n_-(n_e)$  obtained by setting  $dn_-/dt = 0$ . Again, "below" the dot-dashed line,  $dn_-/dt$  is positive. The crossing of the two  $n_-(n_e)$  curves gives the equilibrium. An examination of a small departure from the equilibrium will convince the reader that the equilibrium can be unstable only if both slopes obtained from the  $dn_e/dt = 0$  and  $dn_-/dt = 0$  curves are positive at the crossing, and it is sufficient for instability if the slope of the  $dn_e/dt$  curve is larger. For the example shown in figure 4d we would therefore predict unstable behaviour. Superimposed on figure 4d is the actual trajectory in the phase plane, for

which the complete time-dependent equations are solved. The intersection of the dynamical phase space trajectory with the  $dn_e/dt = 0$  curve indicates the stabilization of the falling electron density.

To explore the details of the bifurcation we need to examine the dynamical behaviour in the transition regions between stability and instability. We do this for small variations of power near the capacitive-to-inductive transition. With increasing power where the  $dn_e/dt = 0$  curve intersects the  $dn_-/dt = 0$  curve near its minimum, the trajectory goes through a series of steps, as shown in figure 4. In figure 4a the motion is stable, collapsing to the fixed point. In figure 4b the bifurcation has occurred, leading to a periodic solution that grows out of the fixed point. In figure 4c the motion has become more complicated with a larger amplitude oscillation appearing somewhat randomly, which is often seen in certain types of chaotic dynamics [10, Sec. 7.5]. Finally, in figure 4d the attractor of the large amplitude relaxation oscillation has been established.

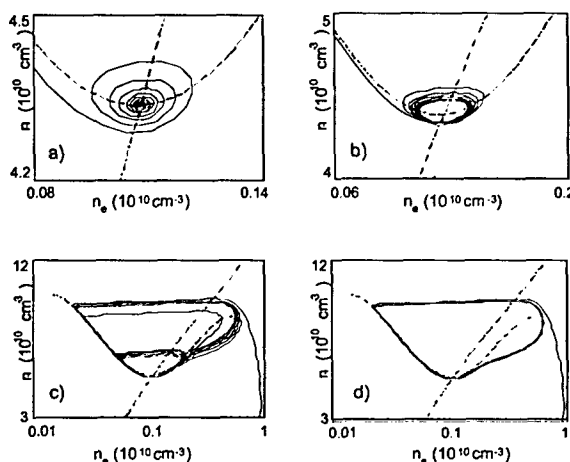


Figure 4: Trajectories when increasing power near the capacitive-to-inductive transition.

### 4. References

- [1] R.A. Hass, Phys. Rev. A **8**, 1017 (1973)
- [2] W.L. Nighan and W.J. Wiegand, Phys. Rev. A **10**, 922 (1974)
- [3] A.D. Barkalov and G.G. Gladush, Sov. Phys. Tech. Phys. **24**, 1203 (1979)
- [4] E. Metsi, E. Gogolides, A. Boudouvis, Phys. Rev. E, **54**, 782 (1996)
- [5] M. Tuszewski, J. Appl. Phys. **79**, 8967 (1996)
- [6] M.A. Lieberman, A.J. Lichtenberg, and M.A. Marakhtanov, Appl. Phys. Lett. **75**, 3617 (1999)
- [7] I.M. El-Fayoumi, I.R. Jones, and M.M. Turner, J. Phys. D **31**, 3082 (1998)
- [8] M.A. Lieberman and R.W. Boswell, J. Phys. IV **8**, Pr7 (1998)
- [9] P. Chabert, A.J. Lichtenberg, M.A. Lieberman, and M.A. Marakhtanov Plasma Sources Sci. Technol **10** (2001) p.478
- [10] A.J. Lichtenberg and M.A. Lieberman, *Regular and Chaotic Dynamics*, 2<sup>nd</sup> Ed. Springer-Verlag, New York, 1992